# Insight Into Cellular Uptake and Transcytosis of Peptide Nanoparticles in a Generalist Caterpillar.

**Erin McGraw**
Department of Biological Sciences, Auburn University
**Jonathan D. Roberts**
Department of Biological Sciences, Auburn University
**Nitish Kunte**
Department of Biological Sciences, Auburn University
**Matthew Westerfield**
Department of Biological Sciences, Auburn University
**Xavier Streety**
Department of Biological Sciences, Auburn University
**David Held**
Department of Entomology and Plant Pathology, Auburn University
**L.Adriana Avila** ( adriana.avila@auburn.edu )
Department of Biological Sciences, Auburn University

**Research Article**

**Keywords:** Cellular Uptake, Transcytosis of Peptide, Generalist Caterpillar

**DOI:** https://doi.org/10.21203/rs.3.rs-293047/v1

# Abstract

Development of novel and specific insect pest management methods is critical for overcoming pesticide resistance and off-target effects. Gene silencing through consumption of double stranded (dsRNA) by insects shows promise in this area. Association of dsRNA with nanoparticles confers protection against nucleases, and can also promote translocation of dsRNA across the midgut epithelial cell membranes, and overall enhance gene knockdown effects. However, many mysteries of how nanoparticles and dsRNA are internalized by cells and subsequently transported across the midgut epithelium remain to be unraveled. In this article, we investigate the role of endocytosis and transcytosis in the uptake and transport of dsRNA and nanoparticles through midgut epithelium cells. *Spodoptera frugiperda* (Sf9) cells and branched amphiphilic peptide nano-capsules (BAPCs) were used as an experimental model. Additionally, analyses of reactive oxygen and nitrogen species (ROS/RNS) were performed to demonstrated that cell viability was minimally impacted by the BAPCs-dsRNA complex. Results suggests that clathrin-mediated endocytosis and macropinocytois are largely responsible for cellular uptake, and once within the midgut, transcytosis is involved in shuttling BAPCs from the lumen to the hemolymph. BAPCs were not found to be toxic to Sf9 cells or generate damaging reactive species once internalized. This opens up further possibilities for BAPCs as a new insect pest management method.


# 1. Introduction

Improvement of pest management approaches is essential for overcoming pesticide resistance and avoid collateral damage to beneficial species.[1] Silencing genes in insects by introducing double-stranded RNA (dsRNA) in the diet holds promise in this field since dsRNA can inhibit translation of vital genes and trigger cell death.[2] Additionally, dsRNA is inexpensive to manufacture and is designed to target specific transcripts with great fidelity without affecting other species.[3] Although this technology has great potential, major drawbacks of dsRNA include instability in the environment, potential degradation by salivary and gut nucleases, and poor uptake by midgut epithelium.[3] Association of dsRNA with cationic nanoparticles can help to overcome these barriers since nanoparticles can shield dsRNA from nucleases and degradative environmental conditions. Nanoparticles can also promote translocation of dsRNA across the midgut epithelial cell membranes.[4]

Our research team developed branched amphipathic peptide capsules (BAPCs) that can be associated with dsRNA and enhance gene silencing when ingested.[5] BAPCs are formed through the assembly of two branched amphipathic peptides $(Ac\text{-}FLIVI)_2\text{-}K\text{-}K_4\text{-}CO\text{-}NH_2$ and $(Ac\text{-}FLIVIGSII)_2\text{-}K\text{-}K_4\text{-}CO\text{-}NH_2$ in water.[6] We have named them “peptide capsules” to avoid confusion with traditional liposomes. In previous studies, Red flour beetle (*Tribolium castaneum*) larvae and adult pea aphids (*Acyrthosiphon pisum*) diets were supplemented with BAPC-dsRNA complexes. The aim was to knockdown BiP and Armet, two genes involved in the unfolded protein response (UPR), and suppressing their translation did result in lethality for both species.[5] For the pea aphid, consumption of BiP-dsRNA associated with BAPCs led to the premature death of the aphids (t1/2= 4–5 days) compared to ingestion of the same amounts of free BiP-

dsRNA (t1/2= 11–12 days). Around 75% of red flour beetles treated with combinatorial treatments (BiP-dsRNA and Armet-dsRNA complexed with BAPCs) died as larvae or during hatching. Feeding both aphids and beetles with dsRNA alone resulted in fewer deaths (~30%). Food regimens containing exclusively BAPCs did not affect survival rates. The results demonstrated that complexation of dsRNA with BAPCs enhanced the oral delivery of dsRNA over dsRNA alone.[6]

In the present study, we investigated the possibility of transcytosis being involved in BAPCs transport across the insect midgut epithelium after ingestion. Transcytosis, commonly used by viruses and proteins to move within tissues, is a vesicle-mediated transport of particles through the interior of the cells followed by ejection from the other side of the cell.[7] It is unknown if this pathway plays a role in the translocation of nanoparticles across the midgut epithelium to access the hemocoel. To mimic ingestion of BAPCs and elucidate if transcytosis is involved in the translocation across the midgut epithelium, midguts of 6$^{th}$ instar *S. frugiperda* larvae were mounted into an Ussing chamber with biological buffers and rhodamine-labeled BAPCs (Rh-BAPCs).[8] Experiments were performed both with and without transcytosis or endocytosis inhibitors, and fluorescence was recorded in the lymph and hemolymph compartments. Our findings indicate that transcytosis contributes to the transport of BAPC across *S. frugiperda* midgut tissue.

Additionally, we explored the specific endocytic routes involved in the cellular internalization of BAPCs with and without dsRNA in *S. frugiperda* cells (Sf9). Endocytosis is one of the major routes by which midgut epithelium cells can uptake dsRNA from midgut lumen.[9] Broadly, this process can be classified as clathrin-dependent or clathrin-independent, and clathrin-independent pathways can be subsequently classified as caveolae-dependent endocytosis, clathrin- and caveolae-independent endocytosis, and micropinocytosis.[10] To date, the best documented endocytic pathway in insects is the clathrin-dependent pathway.[11] Although endocytosis of dsRNA associated with nanoparticles has been studied extensively in mammalian cells, details of those particular pathways in insect cells remains largely unknown.[12] To probe the dependency of BAPC nanoparticles on different endocytic routes, we exposed Sf9 cells to BAPCs and BAPC-dsRNA complexes in the presence of selective endocytic inhibitors. Confocal analysis demonstrated that clathrin-dependent endocytosis and micropinocytosis are the predominant uptake pathways used by BAPC-dsRNA complexes to access the cytosol of Sf9 cells.

Lysosome co-localization experiments were also performed, to evaluate the fraction of BAPCs-dsRNA trapped within this degradative sub-cellular organelle. Production of reactive oxygen and nitrogen species was also analyzed, to ensure that the BAPC-dsRNA did not generate oxidative stress in cells, which could affect off-target species.

# 2. Methods

*Chemical reagents and cell lines*

Sf9 insect Cells (Novagen), 6$^{th}$ instar *S. frugiperda,* 2,2,2-trifluoroethanol (TFE), 6-well TC treated tissue culture plates, Rhodamine B, Grace's Insect Medium 1x supplemented (Thermo Fisher, USA) (Thermo Fisher, USA), fetal bovine serum, chlorpromazine, dynasore, nystatinmethyl-β-cyclodextrin, cytochalasin D, brefeldin A (BFA), 7-AAD, paraformaldehyde, 7AAD, paraformaldehyde,, dsRNA (RNA Greentech, USA), Griess reagent kit for nitrite quantification (Invitrogen, USA), CellROX™ Deep Red (Invitrogen, USA), and Cell Navigatior$^{TM}$ Lysosome Staining Kit- Green Fluorescence (AAT Bioquest, Sunnyvale, CA).

*Synthesis of BAPCs*

The peptides bis(FLIVI)-K-$K_4$ and bis(FLIVIGSII)-K-$K_4$ were synthesized as previously described.[13] To determine each peptide's concentration, they were separately dissolved in 2,2,2-Trifluoroethanol (TFE) and the absorbance of phenylalanine (two per sequence) at 257.5 nm was measured. In TFE, both peptides are helical and monomeric, thereby ensuring complete mixing when combined. After calculating concentrations, the peptides were then mixed at equimolar ratios to generate a fixed calculated concentration of 0.1 mM in the final volume(s), then dried in vacuo. BAPCs were formed by hydrating dried peptides at 25°C and allowed to stand for 10 minutes before solution was cooled and incubated at 4°C for 1 h.[14] After 1 h, the peptide sample was returned to 25°C for 30 min before drying for long-term storage or mixing with the dsRNA.

*Preparation of Rhodamine labeled BAPCs (Rh-BAPCs)*

Rh-BAPCs were prepared similarly to the normal BAPCs, with slight variation. The bis(FLIVI)-K-$K_4$ component of the mixture was modified by the incorporation of N-Hydroxysuccinimide ester of Rhodamine B.[13] Only 25% of the Rhodamine labeled peptide was incorporated in the BACPs. Thus, the final peptide mixture consisted of equimolar concentrations of bis(Ac-FLIVIGSII)-KKKKK-$CONH_2$ and bis(FLIVI)-K-$K_4$ (25% Rh-labeled and 70% unlabeled). As previously described, the peptide mixture was then dissolved in water and incubated at room temperature for 10 min, then kept at 4°C for 1 h. After 1 h, the peptide sample was returned to 25°C for 30 min before drying for long-term storage or mixing with the dsRNA.

*Synthesis of dsRNA*

dsRNA sequence targeting CYP-450 gene in *Popillia japonica* was designed and obtained from RNA Greentech LLC, Texas, USA. First, mRNA sequence of CYP-450 (*P. japonica*: GARJ01000597) were obtained from NCBI nucleotide database. The selected gene sequence was further screened through GenScript siRNA target finder tool to predict siRNA sequences. The sequence region with highest predicted siRNAs was selected for dsRNA synthesis. Sequences from *S. frugiperda* were not selected for dsRNA design to fully explore potential off-target effects.

*Preparation of BAPC-dsRNA complexes*

To form the BAPCs-dsRNA complexes, 200 µL water solutions containing 1 µg of CYP-450 dsRNA were added drop-wise to 200 µL solutions containing 400 µM BAPCs or Rh-BAPCs. Solutions were then mixed carefully by pipette and allow to stand for 10 min before adding $CaCl_2$ at that yielded 1.0 mM final concentration. After 30 min incubation, the solutions containing BAPC-dsRNA complexes were ready for cellular uptake and transcytosis experiments.

*Dynamic light scattering (DLS), Zeta potential (ZP) and Transmission electron microscopy (TEM) analysis*

BAPC-dsRNA complexes were formed by mixing 50, 100, and 120µM BAPCs with 1µg of dsRNA. BAPCs were prepared following the protocol previously described. The particle sizes and zeta-potentials of BAPCs and BAPC-dsRNA complexes were determined using a Zetasizer Nano ZS (Malvern Instruments Ltd., Westborough, MA). Samples were analyzed in 1.0 mM $CaCl_2$ and all measurements were performed in triplicates. For TEM analysis, 40mM of BAPCs mixed with or without 1mg dsRNA were added directly onto individual grids (FCF 300-Cu, Formvar ® carbon film on a 300-mesh copper grid, Electron Microscopy Sciences, Hatfield, PA, USA) and allowed to dry for 2 h at room temperature. Next, samples were negatively stained using phosphotungstic acid and allowed to dry for additional 1 h. TEM imaging was performed at 60 kV on a Zeiss EM10.

*Sf9 Cell Cultures and Growth Conditions*

Sf9 cells were grown in supplemented Grace's Insect Media supplemented with 10% fetal bovine serum with no addition of antibiotics. Cell cultures were grown at 28$^{o}$C and ambient $CO_2$. Adherent cultures were passaged every fourth to fifth day by pipetting media gently across the growth surface until cells were homogenously in solution, and then were transferred to a new T25 flask at $1x10^6$ cells/mL. The media was replaced every 48 h with no addition of antibiotics.

*Endocytosis inhibition study*

Sf9 cells were seeded in 6-well plates containing glass coverslips at a concentration of $1x10^6$ cells/mL and incubated for 36 h at 28°C. Subsequently, media was removed, cells were washed with PBS and inhibitors of endocytosis were added in fresh media at their respective concentrations. Concentrations of inhibitors are as follows: MBCD at 5 mM, CPZ at 10 uM, dynasore at 80 mM, Cytochalasin D at 4 mM, and Nystatin at 50 mM. This inhibitor pretreatment was carried out for 30 min at 28°C. After inhibitor pretreatment, nanoparticles tagged with fluorescent rhodamine dye (Rh-BAPCs) were added to the wells at a concentration of 50 µM and incubated for 1 h at 28°C. Cells were washed once with PBS and then fixed for 15 min with 4% paraformaldehyde, followed by one more PBS wash. Coverslips were removed from the 6-well plates and mounted to microscope slides using ProLong$^{TM}$ Diamond Antifade Mountant. Fluorescent imaging was carried out using the Nikon A1R Confocal Microscope. The same protocol was used for endocytic analysis of BAPC-dsRNA complexes with Rh-BAPCs being conjugated with dsRNA.

*Determination of Reactive Nitrogen Species (RNS) and Reactive Oxygen Species (ROS)*

Reactive Nitrogen Species (nitric oxide species) was detected using the Griess Reagent Kit for Nitrite Determination from Invitrogen. Cells were seeded in 96-well plates at a concentration of $1x10^6$ and incubated for 48 h at 28°C. Cell media was removed and cells were washed with PBS. After inhibitor pretreatment, BAPCs nanoparticles or BAPC-dsRNA complexes were added to the wells at a concentration of 50, 100 and 120 μM and incubated for 1 h at 28°C. Cells were then treated with the Griess reagent as per kit instructions. A standard curve was created by diluting the provided nitrite solutions to final concentrations of 0, 1, 5, 10, 20, 30, 40, and 50 μM. Absorbance at 548 nm was read using automatic plate reader BioTek Cytation3.

The presence of ROS was detected using CellROX™ Deep Red Reagent. Cells were seeded in 96-well plates containing glass coverslips at a concentration of $1x10^6$ and incubated for 48 h at 28°C. Media was removed, cells were washed with PBS, and inhibitors of endocytosis were added in fresh media at their respective concentrations, listed previously. Inhibitor pretreatment was carried out for 30 min at 28°C. After inhibitor pretreatment, BAPC nanoparticles were added to the wells at a concentration of 50 μM and incubated for 1 h at 28°C. Subsequently, cells were incubated with CellROX™ Deep Red Reagent (640/655nm) at a final concentration of 5 μM and protected from light for 30 min at 28°C. Fluorescence was read at 655 nm.

*Cytotoxicity experiment using flow cytometry*

Sf9 cells were seeded in 12-well plates at a concentration of $1x10^6$ cells/mL and incubated for 36 h at 28°C. Cell media was then removed, and media with BAPCs or BAPC-dsRNA complexes at 50, 100 or 120 μM was added were added into the appropriate wells at the concentration previously listed. Same protocol was followed for the endocytosis inhibitors, using the concentrations previously listed. The plates were then incubated for 30 min at 28°C. Cells were incubated an additional hour then washed with PBS and detached from the wells by pipetting. After centrifugation at 1700 rpm for 5 min, cells were resuspended in PBS and 7-AAD was added to detect and exclude dead cells. A total of 10,000 events per sample were analyzed using a MACSQuant® Analyzer 10, Miltenyi Biotec. Side scatter vs. forward scatter gating method was used to eliminate debris and cell clumps. A full gating strategy is shown in **Fig. S1**. Data was analyzed using FlowLogic (Miltenyi Biotec) software.

*Lysosome co-localization*

Cells were seeded in a 6-well plate containing sterile glass coverslips at $1x10^6$ cells/mL and incubated for 36 h at 28°C. Cell media was removed, and cells were washed with PBS. The working solution of Cell Navigator™ was prepared as according to kit instructions. A 1:1 ratio of cell media to Cell Navigator solution was added to the wells, and cells were incubated 2 h at 28°C. Rhodamine-labelled BAPCs complexed with dsRNA were added into the wells 30 min before the Cell Navigator solution was removed. Cells were then washed with PBS twice, and coverslips were mounted using ProLong™ Diamond Antifade Mountant (Thermo) and allowed to dry overnight protected from light overnight. Slides were then imaged using the Nikon A1R Confocal Microscope.

*Insect rearing*

*Spodoptera frugiperda* (fall armyworm) eggs placed in individual growth containers were obtained from Benzon Research (Carlisle, PA, USA). Larvae were reared on a provided wheat germ and soy flour-based artificial diet in a growth chamber at 29°C with a 12:12 (L:D) photoperiod. Larvae were grown until reaching $6^{th}$ instar, then were selected for Ussing chamber experiments.

*Midgut isolation*

Larvae were selected after reaching $6^{th}$ instar but before pupation for dissection. Dissections were performed in insect physiological solution (47 mmol/L KCl, 20.5 mmol/L $MgCl_2$, 20 mmol/L $MgSO_4$, 1 mmol/L $CaCl_2$, 88 mmol/L Sucrose, 4.3 mmol/L $K_2HPO_4$, 1.1 mmol/L $KH_2PO_4$, adjusted to pH 7.5) at room temperature.[15] The midgut was exposed by creating a longitudinal incision on the ventrolateral side. The midgut was isolated and stabilized between two pins before opening it longitudinally. The procedure was done carefully to avoid puncturing, as perforation of the midgut will result in diffusion of particles between chambers rather than active transport. Once opened, the gut was rinsed with insect physiological solution to remove debris then immediately mounted on a modified 0.1 $cm^2$ slider (**Fig. S2**) with great care to conserve lumenal and hemolymphatic orientation.

*Transcytosis experiments ex vivo (pending)*

Midguts mounted in sliders were inserted into an Ussing chamber (Physiologic Instruments, San Diego, CA, USA; Model P2300), **Fig. S2**. The tissue was perfused with 2-3mL lumenal buffer r (5 mmol/L $CaCl_2$, 24 mmol/L $MgSO_4$, 20 mmol/L potassium gluconate, 190 mmol/L sucrose, 5 mmol/L CAPS, pH 10.0) on the lumen side of the midgut, and 2-3mL of hemolymph buffer ((5mmol/L $CaCl_2$, 24 mmol/L $MgSO_4$, 20 mmol/L potassium gluconate, 190 mmol/L sucrose, 5 mmol/L Tris, pH 7.0) on the hemolymphatic side. Air was bubbled gently to each side of the tissue using a fish tank bubbler. Experiments were run at 25°C protected from light. Rhodamine-labelled BAPCs and labelled BAPC-dsRNA complexes were added to the lumenal buffer and 100 µL samples were taken at 0, 15, 30, 45, 60, and 90 min from both sides. Transcytosis-specific inhibitor BFA (10µM) and endocytosis inhibitor CPZ (10 µM) was added 30 min prior to adding BAPCs or complexes. Samples were loaded in a dark-sided 96-well plate and analyzed using a BioTek Cytation 3 plate reader (excitation 544 nm, emission 576 nm). Change in relative fluorescence over time was plotted to visualize the subsequent fluctuation of relative fluorescence due to transcytosis.

*Confocal Laser Scanning Microscopy*

Images were obtained using a confocal LSM 700 laser scanning microscope (Carl Zeiss, Gottingen, Germany).

*Software and Statistical Analyses*

Statistics were performed using GraphPad Prism 5 software (GraphPad Software, La Jolla, CA). A minimum of two replicates were performed for all conditions. Figures were created using biorender.com and Adobe Photoshop CC 2019.

# 3. Results And Discussion

*Biophysical Characterization of BAPC-dsRNA complexes*

BAPCs are formed by mixing the two peptides $(Ac\text{-}FLIVI)_2\text{-}K\text{-}K_4\text{-}CO\text{-}NH_2$ and $(Ac\text{-}FLIVIGSII)_2$-K-K4-CO-NH2 at equimolar concentrations in water, which then co-assemble into 20-100 nm nanoparticles that are resistant to detergents, proteases, and chaotropes.[6,16] BAPCs have unusual but highly desirable properties for oral delivery of dsRNA in insects, such as side chains with pKa values between 9 to 13.[4] Nanoparticles with these functional groups are more stable in neutral and alkaline midgut environments of some species such as *Spodoptera exigua*, which is characterized for being recalcitrant to dsRNA effects[3]. BAPCs can also act as cationic nucleation centers that bind electrostatically with plasmid DNA, generating BAPC-DNA complexes with sizes ranging from 50 to 250 nm.[14] In this study, we sought to address the size and structure of the BAPCs associated with a 252 bp dsRNA. Transmission electron microscopy (TEM) analysis revealed that similar to DNA, the dsRNA surrounds the cationic surface of the BAPCs, yielding a BAPC-dsRNA complexes of 50-200 nm size (**Fig. 1A, B, C**). These results are in accordance with the size previously observed for similar BAPCs and BAPC-dsRNA formulations using Atomic Force Microscopy (AFM).

To expand the biophysical analysis of the BAPC-dsRNA complexes, we also performed Dynamic Light Scattering analysis (DLS).[17] This technique is used for the determination of the hydrodynamic diameter of nanoparticles dispersed in a liquid medium by measuring changes in the intensity of the scattered light[17]. The hydrodynamic diameter will depend not only on the size of the particle “core”, but also ions present on the surface. In general, particles with a larger hydrodynamic diameter scatter much more light than small particles.[18] Different BAPCs and dsRNA formulations were analyzed by DLS by keeping the amount of dsRNA constant (1 µg) and varying the BAPCs concentration (**Fig. 1D**). The BAPC-dsRNA complexes displayed larger hydrodynamic diameter than the bare BAPCs. The increase in size after association with dsRNA also indicates that the complexes are tightly bound as they do not readily dissociate upon dilution.

Finally, we analyzed the zeta potential (ZP) of BAPCs and the BAPC-dsRNA complexes (**Fig. 1E)**. ZP is a measure of the magnitude of the electrostatic charge or repulsion/attraction between particles and is one of the fundamental parameters known to affect stability.[19] Positive ZP values might enhance electrostatic interactions with the negatively charged cell membranes.[14,19] However, values above 45 mV can trigger high levels of toxicity.[20,21] To investigate the ZP values of BAPCs and the BAPC-dsRNA complexes, different concentrations of BAPCs were analyzed both alone and complexed with 1 µg dsRNA. BAPCs showed ZP values of ~40 mV and this value decreased to ~10 mV after association with

dsRNA, confirming TEM analysis results that the dsRNA surrounds the peptide nanocapsules, thus altering the surface charge. Despite varying BAPC concentrations, the overall surface charge of the BAPC-dsRNA complexes remained positive, which facilitates interaction with negatively-charged cell membranes.

*Cellular Uptake Mechanisms and Lysosome Co-localization of BAPCs and BAPC-dsRNA complexes*

Literature suggests that nanoparticles can be internalized by cells through two pathways: non-endocytic and endocytic. Non-endocytic pathways involve a passive penetration of the plasma membrane.[12] Endocytic pathways are energy dependent and can be divided in phagocytosis (large size), pinocytosis (small size), and receptor-mediated.[10] Pinocytosis can be further classified into four specific pathways depending on the proteins involved in the internalization process: clathrin-mediated, caveolin-mediated, clathrin- and caveolin-independent, and macropinocytosis.[10] Previous studies conducted in mammalian cells demonstrated that micropinocytosis, clathrin-dependent, and caveolae-dependent endocytosis are primarily responsible for BAPC internalization.[22]

In this article, we seek to elucidate endocytic pathways involved in BAPC and BAPC-dsRNA complex uptake in insect cells. To accomplish this goal, we incubated Sf9 cells with Rh-BAPCs in the presence of selective endocytic inhibitors.[23] Subsequently, cellular internalization was monitored qualitatively using confocal microscopy. A list of all inhibitors used and their mode of action is listed in **Table 1**.

**Table 1. Inhibitors used in the study of BAPCs internalization and transport.**

| Endocytic Pathway | Inhibitor | Mode of inhibition | Ref |
|---|---|---|---|
| **Clathrin-mediated** | chlorpromazine | Sequesters clathrin and AP2 from the cell membrane | 24, 25 |
| | dynasore | Inhibits dynamin and polymerization of actin | 24, 25 |
| **Caveolae-mediated** | methyl-b-cyclodextrin | Extracts cholesterol from plasma membrane | 25 |
| | nystatin | Extracts cholesterol from plasma membrane | 25 |
| **Macropinocytosis** | cytochalasin D | Caps and prevents assembly of actin | 24,25,26 |
| **Transcytosis** | brefeldin A | Disrupts regulation and creation of Golgi vesicles | 27 |

Our results indicate that clathrin-mediated and macropinocytosis are the major endocytic routes employed by BACPs to access the cytosol of Sf9 cells. Notably, for the BAPC-dsRNA complexes, the caveolae/lipid raft dependent endocytosis seemed to also play a role in the cellular internalization process (**Fig. 2**). Several nanomaterials that have shown successful delivery use macropinocytosis since

it forms a large leaky vesicle that can enclose several nanoparticles.[28] Therefore, it was expected that this pathway was involved in the uptake of BAPCs. Review of literature suggests that one cell type can sometimes endocytose the same nanoparticle using multiple pathways, as nanoparticle formulations are often made up of a group of heterogeneous particles with different sizes, which makes the uptake process more diverse.[29] Clathrin-mediated endocytosis, micropinocytosis and caveolin-mediated endocytosis have been documented before in insect cells, including Sf9 cells for the uptake of dsRNA, viruses, proteins and lipoproteins.[30,31,32,33,34] Nonetheless, this is the first study that demonstrates the implication of these pathways in the internalization of dsRNA and dsRNA associated with peptide nanoparticles.

After cellular entry, internalized nanoparticles are delivered to the early endosome. Subsequently, the early endosomes undergo a maturation process that ultimately results in the formation of the endolysosome, a temporary hybrid organelle resulting from fusion with lysosomes (**Fig. 3A**).[12] Lysosomes are the final destination for external macromolecules and nanoparticles.[35] The lysosomal lumen has an acidic pH close to 4.5 and contains approximately 60 different soluble

hydrolytic enzymes, thus macromolecules and nanoparticles trapped within these organelles are often degraded.[36] Success in gene silencing through dsRNA is often hindered by the entrapment and subsequent degradation of these molecules in this acidic compartment. This degradation process contributes to what is known as dsRNA resistance, and it has been a barrier for the development of broader applications of dsRNA-based technology in insects.[9]

To evaluate the entrapment of the BAPC-dsRNA complexes within the lysosomes; BAPCs prepared with a 25% rhodamine B and complexed with dsRNA were incubated with Sf9 cells for 1 h. Lysosomes were stained using Cell Navigator™. As shown in **Fig. 3**, rhodamine B labeled BAPCs-dsRNA complex (**Fig. 3B**) and the stained lysosomes (**Fig. 3C**) are visualized in the Sf9 cells. Upon merging with bright field (**Fig. 3D),** the two images show only a small fraction of the labeled BAPCs-dsRNA appeared to be co-localized within the lysosome (**Fig. 3E**). These results suggest that BAPC-dsRNA complexes are processed by the endosomal route yet rapidly escape the late endosomes or endolysosome. Most likely, the amine groups found on the hydrophilic tails of BAPC peptides trigger the rupture of the endosomes by osmotic pressure.[37] Once ruptured, the complexes are released into the cytosol, thus avoiding entrapment and degradation in acidic lysosomes, previously identified as a source of failure of dsRNA in lepidopterans.[35,38]

*BAPC-dsRNA transport across the midgut epithelium*

Following ingestion by a host, the BAPCs are taken up by the midgut epithelium cells and potentially spread through the whole insect body. Gene knockdown and gene expression analysis in some insect species have demonstrated the role of the SID-1 like (Sil) channel protein in dsRNA uptake. In such species, this channels are also involve in the translocation within the midgut tissue.[7,39,40,41,42,43,44] Nonetheless, the transport mechanism is largely unknown for nanoparticles.[4,45] A better understanding

of how these macromolecules cross the insect midgut will help to more effectively utilize currently available dsRNA-based technology and improve the development of novel insecticide delivery methods.[4]

To elucidate how BAPCs translocate midgut epithelium cells, midguts of 6$^{th}$ instar *S. frugiperda* larvae were exposed to Rh-BAPCs for over a period of 90 min in an Ussing chamber. (**Fig 4A**). BFA was used to study the potential role of transcytosis from the midgut lumen to the hemolymph. BFA is a selective transcytosis inhibitor previously studied in mammalian cells that impacts the regulation and creation of Golgi transport vesicles.[26] CPZ was also used to study how endocytosis inhibition impacted transcytosis. Rh-BAPCs in the absence of any inhibitors showed evident transcytosis (**Fig. 4 B, C**). Nanoparticles were added into the lumenal side. Over time, transcytosis moved Rh-BAPCs into the hemolymph compartment, thus increasing the relative fluorescence of that compartment. If active transport was not involved, the nanoparticles would have remained within the tissue, not increasing the relative fluorescence of the hemolymph buffer. The relative fluorescence seen in the hemolymph increased significantly after a period of 90 min, suggesting the occurrence of complete transcytosis (**Fig 4. C**).

The addition of inhibitors appeared to decrease fluorescence in the hemolymph side compared to the levels of the BAPCs treated group (**Fig 4C**). This suggests that there is an inhibition of transcytosis from both brefeldin A and CPZ. This also confirms previous results of clathrin-mediated endocytosis playing a major role in BAPCs internalization, thus impacting transcytosis. Similar results should be expected for BAPC-dsRNA complexes, since alike endocytosis, transcytosis is a vesicular-mediated pathway[8,45]. Nonetheless, future studies will address the specific role of transcytosis in the presence of dsRNA targeting different genes, and the role of the SID-1 like receptors in nanoparticle translocation.

*Cytotoxicity of BAPCs and BAPC-dsRNA complexes in insect cells*

In order to ensure potential field applications of dsRNA-based technology, it is essential to understand the potential cytotoxic effects of the peptide nanoparticles and dsRNA in non-target organisms. By using Sf9 as insect cell model and the non-specific dsRNA targeting *P. japonica*, we evaluated the generation of reactive oxygen species (ROS) by cells in response to BAPCs and BAPC-dsRNA complexes. The generation of ROS can trigger lipid peroxidation, thus destabilizing the cell membrane and making it more susceptible to further oxidation. ROS can also damage DNA and disrupt mitochondrial activity. [46,47] Although it is more common observed in metallic nanoparticles, measuring ROS of BAPCs in Sf9 cells will help us determine potential downstream effects from a toxicity perspective. ROS was detected using the CellROX™ Deep Red fluorescence assay.[48] The release of reactive oxygen species causes increase in fluorescence of membrane permeable CellROX. According with the results (**Fig. 5A**), BAPCs did not cause a significant increase in the ROS when compared with untreated cells.

Similar to ROS, reactive nitrogen species (RNS) are naturally occurring within living systems. At low levels they are used by organisms for signaling purposes.[49] However, higher levels of RNS can be detrimental to the cells ultimately leading to cell death. In the instance that ROS and RNS production are both increased, there becomes the danger of creating peroxinitrite which is a potent oxidative agent that can damage

organism DNA.[49,50] The production of RNS in Sf9 cells was quantified using Griess Reagent alongside a standard curve. As show in **Fig. 5B**, there is no significant difference between the control groups (untreated cells) and both BAPCs and BAPC-dsRNA complexes.

Cytotoxicity was evaluated as well by flow cytometry (**Fig. 5C**). This is a rapid and reliable method to quantify cell viability.[51] Dead cells can be identified by using fluorescence probes that bind to DNA of cells with compromised cell membrane. The viability of Sf9 cells treated with 50 to 120 mM of BAPCs with or without dsRNA was minimally affected (<15% cell mortality), but according with the statistical analysis ($p > 0.12$), no significance difference was found when compared with untreated cells. We also analyzed viability in the presence of the endocytosis inhibitors, to ensure that this cell viability was preserved during the treatments. None of the inhibitors caused increase in cell viability or oxidative stress, thus avoiding false positive uptake results produced by damaged cell membranes (**Fig. S3)**. Altogether these results indicate that BAPCs neither induce cell death nor oxidative stress in insect cells. Moreover, studies conducted in mammalian cell lines and animal models also indicated that BAPCs do not induce acute toxicity and are not immunogenic, making them a suitable candidate for field applications for dsRNA delivery.[14]

# 4. Conclusions

A major objective of current pest control methods is protection of crops from economically-damaging species. Due to an increase in pesticide resistance and the potential for off-target effects, delivery of dsRNA has become an attractive option. It has been demonstrated that association of dsRNA with nanoparticles provide protection against nucleases, and can also promote translocation of dsRNA across the midgut epithelial cell membranes, thus enhancing overall gene knockdown effects[4]. Nonetheless, several cellular nanoparticle processing such as uptake, lysosome degradation, toxicity and transport across insect midgut remained largely unknow.

Here we demonstrated that BAPC nanoparticles are able to enter, and subsequently transverse the gut of *S. frugiperda* via an active transport (transcytosis). By using a physiological chamber that mimic in vivo conditions and transcytosis inhibitors, midguts of 6$^{th}$ instar larvae were exposed to fluorescent-labelled BAPCs. Without inhibitors, fluorescence decreased in the luminal compartment and increased in the hemolymph in a time-dependent manner. This indicated that transcytosis was involved in movement of Rd-BAPCs across the midgut. Upon the addition of a specific inhibitor, a significant decrease in fluorescence in the hemolymph after 2 h was observed compared to controls.

The endocytic cellular uptake route of BAPCs and BAPC-dsRNA complexes in Sf9 cells was also studied. We used specific endocytosis inhibitors to individually target micropinocytosis, clathrin-, and caveolae-mediated endocytosis. Confocal analysis indicated that micropinocytosis and clathrin-mediated endocytosis are the major uptake routes involved in BAPC-dsRNA complex internalization. Additionally, our results indicated that once internalized, BAPC-dsRNA escape the endosomal pathway, probably due to a phenomenon called “proton sponge effect”. In this process, the endosomal membrane is destabilized by osmotic pressure.[37] Co-incubation of BAPCs or BAPC-dsRNA complexes did not produce cytotoxic

reactive nitrogen or oxygen species nor cell membrane damage. Excess of either of these cellular stress markers can indicate harm to the cell, and possible cell death to off-target species.

# Declarations


### Funding sources:

This project was supported by the Alabama Agricultural Experiment Station and the Hatch program of the National Institute of Food and Agriculture, U.S. Department of Agriculture.


### Author Contribution statement

E.M. performed lysosome co-localization, toxicity, transcytosis assays. J.R. performed ROS, NOS, and endocytosis studies. N.K. performed toxicity assay, gut dissections, and transcytosis. M.W. performed TEM imaging and analysis, and performed RNS assay. X.S. prepared rhodamine labeled BAPCs and performed TEM imaging and analysis. D.H. assisted in insect rearing and dissections  L.A. wrote the main manuscript text, provided main idea, experimental design and funding. All authors assisted with final manuscript edits.

# References


1. Fletcher, S. J., Reeves, P. T., Hoang, B. T. & Mitter, N. A Perspective on RNAi-Based Biopesticides. *Front. Plant Sci.* (2020) doi:10.3389/fpls.2020.00051.
2. Cooper, A. M. W., Silver, K., Zhang, J., Park, Y. & Zhu, K. Y. Molecular mechanisms influencing efficiency of RNA interference in insects. *Pest Management Science* (2019) doi:10.1002/ps.5126.
3. Zhang, H., Li, H. C. & Miao, X. X. Feasibility, limitation and possible solutions of RNAi-based technology for insect pest control. *Insect Science* (2013) doi:10.1111/j.1744-7917.2012.01513.x.
4. Kunte, N., McGraw, E., Bell, S., Held, D. & Avila, L. A. Prospects, challenges and current status of RNAi through insect feeding. *Pest Management Science* (2020) doi:10.1002/ps.5588.
5. Avila, L. A. *et al.* Delivery of lethal dsRNAs in insect diets by branched amphiphilic peptide capsules. *J. Control. Release***273**, 139–146 (2018).
6. Gudlur, S. *et al.* Peptide Nanovesicles Formed by the Self-Assembly of Branched Amphiphilic Peptides. *PLoS One***7**, (2012).
7. Denecke, S., Swevers, L., Douris, V. & Vontas, J. How do oral insecticidal compounds cross the insect midgut epithelium? *Insect Biochemistry and Molecular Biology* vol. 103 22–35 (2018).
8. Kemmerer, M. & Bonning, B. C. Transcytosis of Junonia coenia densovirus VP4 across the gut epithelium of Spodoptera frugiperda (Lepidoptera: Noctuidae). *Insect Sci.* (2020) doi:10.1111/1744-7917.12600.
9. Yoon, J. S., Gurusamy, D. & Palli, S. R. Accumulation of dsRNA in endosomes contributes to inefficient RNA interference in the fall armyworm, Spodoptera frugiperda. *Insect Biochem. Mol.*

*Biol.***90**, 53–60 (2017).

10. Sahay, G., Alakhova, D. Y. & Kabanov, A. V. Endocytosis of nanomedicines. *Journal of Controlled Release* vol. 145 182–195 (2010).
11. Vélez, A. M. & Fishilevich, E. The mysteries of insect RNAi: A focus on dsRNA uptake and transport. *Pesticide Biochemistry and Physiology* vol. 151 25–31 (2018).
12. Patel, S. *et al.* Brief update on endocytosis of nanomedicines. *Advanced Drug Delivery Reviews* (2019) doi:10.1016/j.addr.2019.08.004.
13. Sukthankar, P. *et al.* Branched amphiphilic peptide capsules: Cellular uptake and retention of encapsulated solutes. *Biochim. Biophys. Acta - Biomembr.* (2014) doi:10.1016/j.bbamem.2014.02.005.
14. Avila, L. A. *et al.* Gene delivery and immunomodulatory effects of plasmid DNA associated with Branched Amphiphilic Peptide Capsules. *J. Control. Release* (2016) doi:10.1016/j.jconrel.2016.08.042.
15. Cermenati, G. *et al.* The CPP Tat enhances eGFP cell internalization and transepithelial transport by the larval midgut of Bombyx mori (Lepidoptera, Bombycidae). *J. Insect Physiol.* (2011) doi:10.1016/j.jinsphys.2011.09.004.
16. Barros, S. D. M. *et al.* Branched Amphipathic Peptide Capsules: Different Ratios of the Two Constituent Peptides Direct Distinct Bilayer Structures, Sizes, and DNA Transfection Efficiency. *Langmuir* (2017) doi:10.1021/acs.langmuir.7b00912.
17. Ramos, A. P. Dynamic Light Scattering Applied to Nanoparticle Characterization. in *Nanocharacterization Techniques* (2017). doi:10.1016/B978-0-323-49778-7.00004-7.
18. Maguire, C. M., Rösslein, M., Wick, P. & Prina-Mello, A. Characterisation of particles in solution–a perspective on light scattering and comparative technologies. *Science and Technology of Advanced Materials* (2018) doi:10.1080/14686996.2018.1517587.
19. Bhattacharjee, S. DLS and zeta potential - What they are and what they are not? *Journal of Controlled Release* (2016) doi:10.1016/j.jconrel.2016.06.017.
20. Shao, X. R. *et al.* Independent effect of polymeric nanoparticle zeta potential/surface charge, on their cytotoxicity and affinity to cells. *Cell Prolif.* (2015) doi:10.1111/cpr.12192.
21. Gumustas, M., Sengel-Turk, C. T., Gumustas, A., Ozkan, S. A. & Uslu, B. Effect of Polymer-Based Nanoparticles on the Assay of Antimicrobial Drug Delivery Systems. in *Multifunctional Systems for Combined Delivery, Biosensing and Diagnostics* (2017). doi:10.1016/b978-0-323-52725-5.00005-8.
22. Natarajan, P. *et al.* A Study of the Cellular Uptake of Magnetic Branched Amphiphilic Peptide Capsules. *Mol. Pharm.* (2020) doi:10.1021/acs.molpharmaceut.0c00393.
23. Vercauteren, D. *et al.* The use of inhibitors to study endocytic pathways of gene carriers: Optimization and pitfalls. *Mol. Ther.* (2010) doi:10.1038/mt.2009.281.
24. Dutta, D. & Donaldson, J. Search for inhibitors of endocytosis: Intended specificity and unintended consequences. *Cell. Logist.* (2012) doi:10.4161/cl.23967.

25. Sato, K., Nagai, J., Mitsui, N., Ryoko Yumoto & Takano, M. Effects of endocytosis inhibitors on internalization of human IgG by Caco-2 human intestinal epithelial cells. *Life Sci.* (2009) doi:10.1016/j.lfs.2009.10.012.
26. Saha, K. *et al.* Surface functionality of nanoparticles determines cellular uptake mechanisms in mammalian cells. *Small* (2013) doi:10.1002/smll.201201129.
27. Hunziker, W., Andrew Whitney, J. & Mellman, I. Selective inhibition of transcytosis by brefeldin A in MDCK cells. *Cell* (1991) doi:10.1016/0092-8674(91)90535-7.
28. Hillaireau, H. & Couvreur, P. Nanocarriers' entry into the cell: Relevance to drug delivery. *Cellular and Molecular Life Sciences* (2009) doi:10.1007/s00018-009-0053-z.
29. Date, A. A., Hanes, J. & Ensign, L. M. Nanoparticles for oral delivery: Design, evaluation and state-of-the-art. *J. Control. Release* (2016) doi:10.1016/j.jconrel.2016.06.016.
30. Hodgson, J. J., Buchon, N. & Blissard, G. W. Identification of insect genes involved in baculovirus AcMNPV entry into insect cells. *Virology* (2019) doi:10.1016/j.virol.2018.10.022.
31. Van Hoof, D., Rodenburg, K. W. & Van Der Horst, D. J. Receptor-mediated endocytosis and intracellular trafficking of lipoproteins and transferrin in insect cells. *Insect Biochem. Mol. Biol.* (2005) doi:10.1016/j.ibmb.2004.09.009.
32. Long, G., Pan, X., Kormelink, R. & Vlak, J. M. Functional Entry of Baculovirus into Insect and Mammalian Cells Is Dependent on Clathrin-Mediated Endocytosis. *J. Virol.* (2006) doi:10.1128/jvi.00880-06.
33. Kunz, D. *et al.* Receptor mediated endocytosis of vicilin in Callosobruchus maculatus (Coleoptera: Chrysomelidae) larval midgut epithelial cells. *Comp. Biochem. Physiol. Part - B Biochem. Mol. Biol.***210**, 39–47 (2017).
34. Mercer, J. & Helenius, A. Virus entry by macropinocytosis. *Nature Cell Biology* (2009) doi:10.1038/ncb0509-510.
35. Paillard, A., Hindré, F., Vignes-Colombeix, C., Benoit, J. P. & Garcion, E. The importance of endo-lysosomal escape with lipid nanocapsules for drug subcellular bioavailability. *Biomaterials* (2010) doi:10.1016/j.biomaterials.2010.06.024.
36. Ballabio, A. The awesome lysosome. *EMBO Mol. Med.* (2016) doi:10.15252/emmm.201505966.
37. Battistella, C. & Klok, H. A. Controlling and Monitoring Intracellular Delivery of Anticancer Polymer Nanomedicines. *Macromolecular Bioscience* (2017) doi:10.1002/mabi.201700022.
38. Shukla, J. N. *et al.* Reduced stability and intracellular transport of dsRNA contribute to poor RNAi response in lepidopteran insects. *RNA Biol.* (2016) doi:10.1080/15476286.2016.1191728.
39. Aronstein, K., Pankiw, T. & Saldivar, E. SID-I is implicated in systemic gene silencing in the honey bee. *J. Apic. Res.* (2006) doi:10.1080/00218839.2006.11101307.
40. Cappelle, K., De Oliveira, C. F. R., Van Eynde, B., Christiaens, O. & Smagghe, G. The involvement of clathrin-mediated endocytosis and two Sid-1-like transmembrane proteins in double-stranded RNA uptake in the Colorado potato beetle midgut. *Insect Mol. Biol.***25**, 315–323 (2016).

41. Luo, Y., Wang, X., Yu, D. & Kang, L. The SID-1 double-stranded RNA transporter is not required for systemic RNAi in the migratory locust. *RNA Biol.* (2012) doi:10.4161/rna.19986.
42. Miyata, K. *et al.* Establishing an in vivo assay system to identify components involved in environmental RNA interference in the western corn rootworm. *PLoS One* (2014) doi:10.1371/journal.pone.0101661.
43. Xu, J. *et al.* Establishment of Caenorhabditis elegans SID-1-dependent DNA delivery system in cultured silkworm cells. *Mol. Biotechnol.* (2014) doi:10.1007/s12033-013-9694-0.
44. Li, X., Dong, X., Zou, C. & Zhang, H. Endocytic pathway mediates refractoriness of insect Bactrocera dorsalis to RNA interference. *Sci. Rep.***5**, (2015).
45. Tomoyasu, Y. *et al.* Exploring systemic RNA interference in insects: A genome-wide survey for RNAi genes in Tribolium. *Genome Biol.* (2008) doi:10.1186/gb-2008-9-1-r10.
46. Manke, A., Wang, L. & Rojanasakul, Y. Mechanisms of nanoparticle-induced oxidative stress and toxicity. *BioMed Research International* (2013) doi:10.1155/2013/942916.
47. Ansari, M. O. *et al.* Evaluation of DNA interaction, genotoxicity and oxidative stress induced by iron oxide nanoparticles both in vitro and in vivo: attenuation by thymoquinone. *Sci. Rep.* (2019) doi:10.1038/s41598-019-43188-5.
48. Patlolla, A. K., Kumari, S. A. & Tchounwou, P. B. A comparison of poly-ethylene-glycol-coated and uncoated gold nanoparticle-mediated hepatotoxicity and oxidative stress in sprague dawley rats. *Int. J. Nanomedicine* (2019) doi:10.2147/IJN.S185574.
49. Di Meo, S., Reed, T. T., Venditti, P. & Victor, V. M. Role of ROS and RNS Sources in Physiological and Pathological Conditions. *Oxidative Medicine and Cellular Longevity* (2016) doi:10.1155/2016/1245049.
50. Hardy, M. *et al.* Detection and Characterization of Reactive Oxygen and Nitrogen Species in Biological Systems by Monitoring Species-Specific Products. *Antioxidants and Redox Signaling* (2018) doi:10.1089/ars.2017.7398.
51. McGraw, E. *et al.* Laser-Assisted Delivery of Molecules in Fungal Cells. *ACS Appl. Bio Mater.* (2020) doi:10.1021/acsabm.0c00720.

# Figures

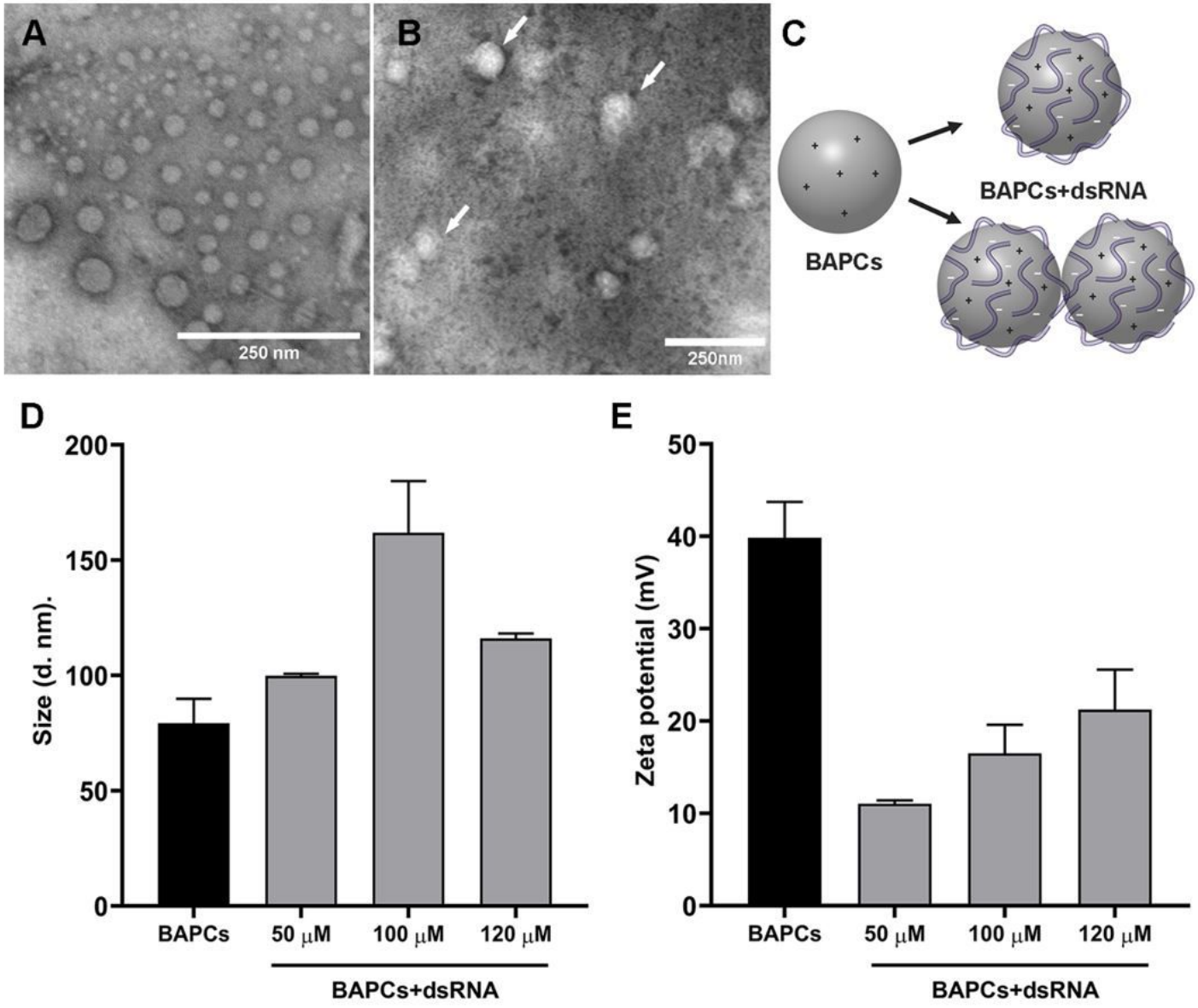


## Figure 1

Biophysical characterization of BAPCs and BAPC-dsRNA complexes. The amount of dsRNA was held constant at 1 □g. A) TEM analysis of BAPCs without and B) with dsRNA. C) Illustration of dsRNA complexing with BAPCs. D) DLS and E) ZP analysis of BAPC-dsRNA complexes.

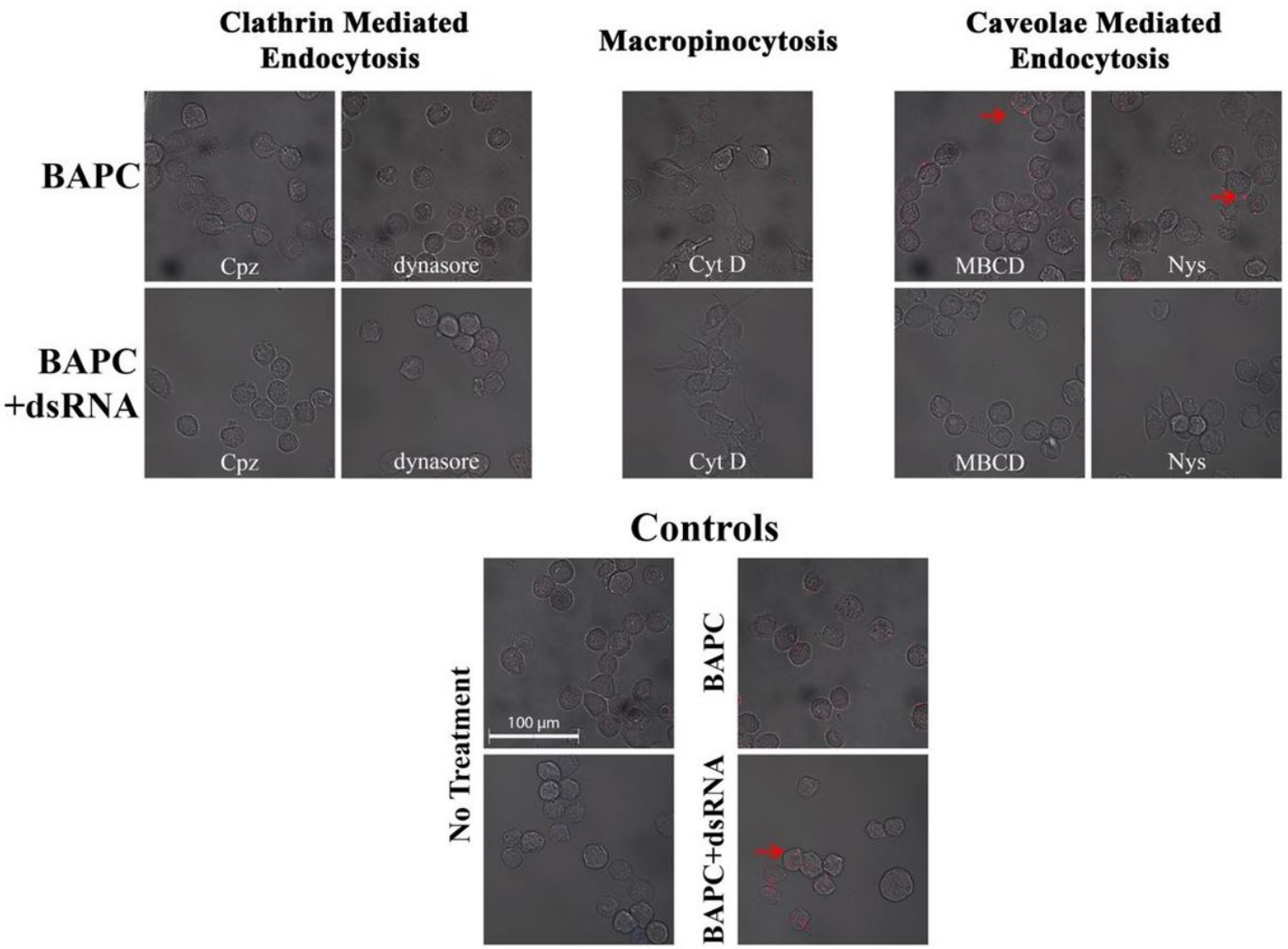


## Figure 2

Endocytosis inhibition assay of BAPC and BAPC+dsRNA in Sf9 cells. BAPCs are labeled with Rhodamine B(red). The change in BAPC uptake as a result of complexation with dsRNA via each endocytosis pathway is shown. Each endocytosis inhibitor is shown in the presence of only BAPCs (upper panel) and BAPCs+dsRNA (lower panel).

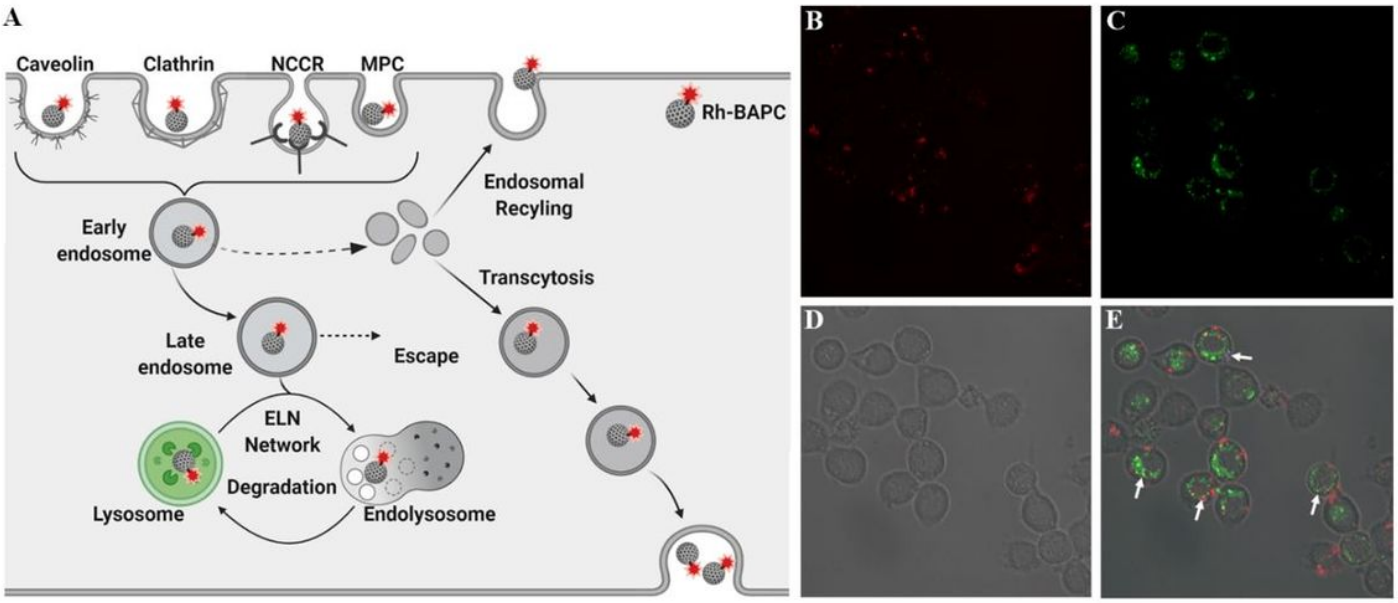


## Figure 3

Colocalization of BAPCs with dsRNA in lysosomes. 2.5µg of dsRNA was complexed with 50µM of BAPCs and incubated with Sf9 cells for 1 h. Lysosomes were stained with Cell NavigatorTM . Confocal microscopy was used to check for colocalization of complexes in lysosomes. A) Schematic representation of endocytic pathways and endosome maturation process. B) Rh-BAPCs (red), C) lysosomes (Green), D) bright field and E) merge image showing co-localization of BAPCs and the lysosomes (yellow).

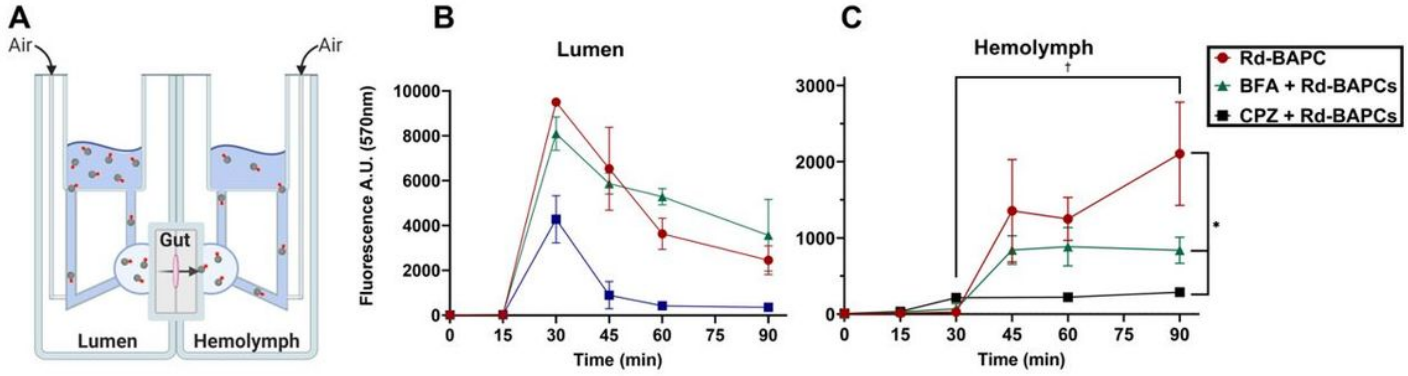


## Figure 4

Transcytosis of Rh-BAPCs through S. frugiperda midgut in the presence of transcytosis and endocytosis inhibitors. A) Scheme showing the movement of Rd-BAPCs through midgut tissue in an Ussing chamber. B) Relative fluorescence of lumenal buffer or C) hemolymph buffer over 90 minutes. Data represent mean values +SD of two experiments combined. Statistical significance: (*) $p < 0.033$; (***) $p < 0.001$; (ns) $p >$

0.12 versus Rd-BAPC control (no inhibitors) or as indicated in the bars (ANOVA, Dunnett posttest). (†) p < 0.033; versus control (t=30min, immediately after BAPC addition) (ANOVA, Dunnett posttest).

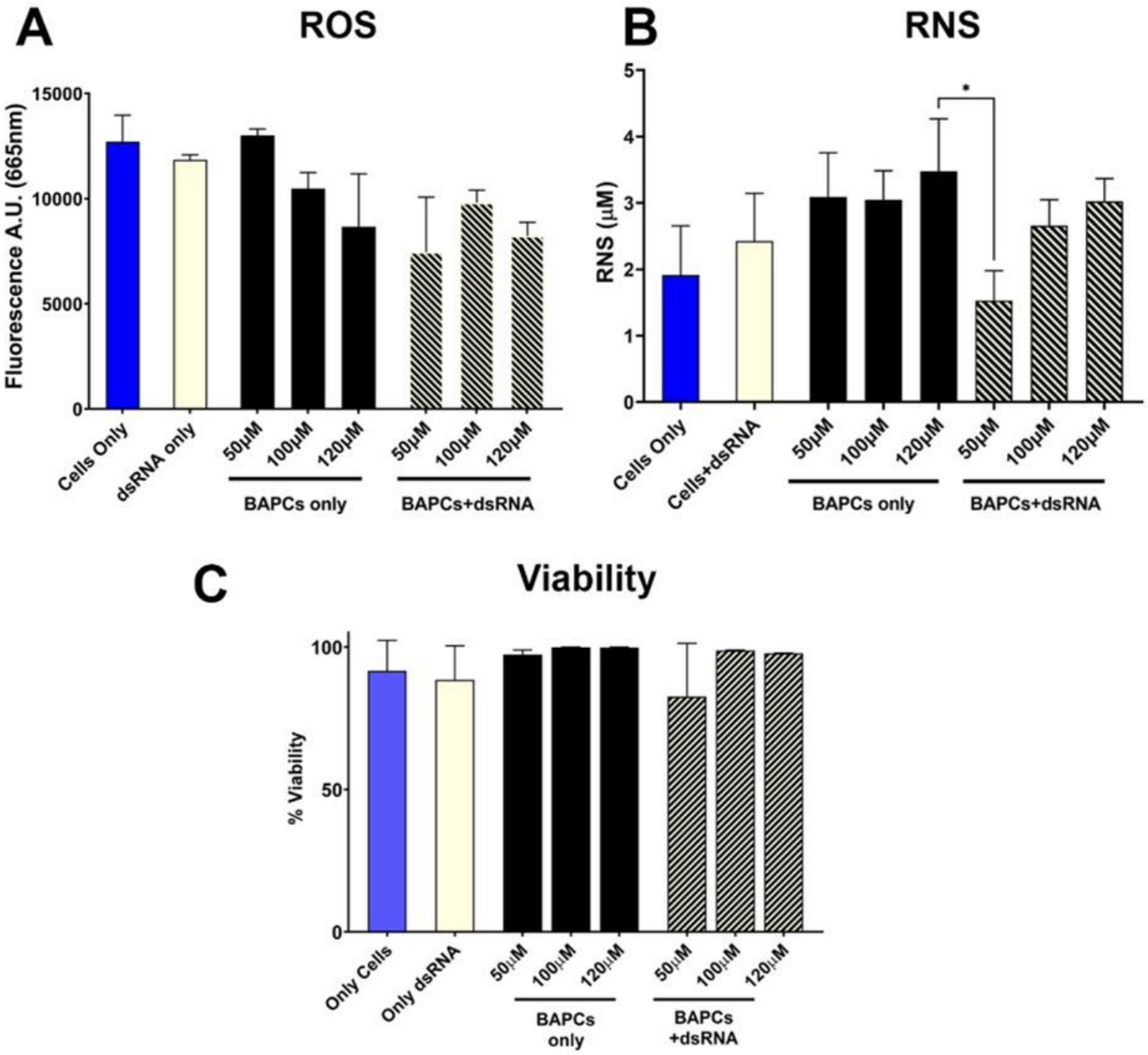


## Figure 5

The effect of BAPC-dsRNA complexes on cell viability and oxidative stress. A) Shows the production of RNS based on treatment group. B) Shows the relative production of ROS based on treatment group. C) Indicates how cell membrane integrity is affected by the different treatment groups by using the dead cell exclusion dye 7-AAD. Data represent mean values +SD of two experiments combined. Statistical significance: (*) p < 0.033; (***) p < 0.001; (ns) p > 0.12 versus groups indicated in the bars (ANOVA, Dunnett posttest).

# Supplementary Files

This is a list of supplementary files associated with this preprint. Click to download.

- SupplementaryInformation.docx